

# Selective hydrogenolysis of bio-renewable tetrahydrofurfurylamine to piperidine on $\text{ReO}_x$ -modified Rh catalysts

*Cheng-Bin Hong, † Guoliang Li † and Haichao Liu\**

† These authors contributed equally to this work.

Beijing National Laboratory for Molecular Sciences, College of Chemistry and

Molecular Engineering, Peking University, Beijing 100871, China.

Email: hcliu@pku.edu.cn

## Contents

### **Experimental section: general procedure for synthesis of N,N,N-trimethyl-1-(tetrahydrofuran-2-yl)methanaminium chloride.**

**Fig. S1** Transmission electron microscopy (TEM) micrographs (scale bar = 20 nm) and histograms of metal particle size distribution for (a) Rh- $\text{ReO}_x/\text{C}$  (2 wt% Rh, 2.2 wt% Re), (b) Rh- $\text{ReO}_x/\text{ZrO}_2$  (2 wt% Rh, 2.2 wt% Re) and (c) Rh- $\text{ReO}_x/\text{Nb}_2\text{O}_5$  (2 wt% Rh, 2.2 wt% Re).

**Fig. S2** Transmission electron microscopy (TEM) micrographs (scale bar = 20 nm) and histograms of metal particle size distribution for Rh- $\text{ReO}_x/\text{SiO}_2$  (2 wt% Rh, (a) 0.1 wt% Re, (b) 0.3 wt% Re, (c) 0.9 wt% Re, (d) 1.4 wt% Re and (e) 2.7 wt% Re).

**Fig. S3** High angle annular dark field scanning transmission electron microscopy (HAADF-STEM) micrographs (scale bar = 20 nm) and electron dispersive X-ray (EDX) microanalyses of Rh- $\text{ReO}_x/\text{SiO}_2$  (2 wt% Rh, (a) 0.1 wt% Re, (b) 0.3 wt% Re, (c) 0.9 wt% Re, (d) 1.4 wt% Re and (e) 2.7 wt% Re).

**Fig. S4** XRD patterns of Rh- $\text{ReO}_x/\text{SiO}_2$  (2 wt% Rh, (a) 0.1 wt% Re, (b) 0.3 wt% Re, (c) 0.9 wt% Re, (d) 1.4 wt% Re, (e) 2.2 wt% Re, (f) 2.7 wt% Re) and (g) the spent Rh-

ReO<sub>x</sub>/SiO<sub>2</sub> (2 wt% Rh, 1.4 wt% Re).

**Fig. S5** Transmission electron microscopy (TEM) micrographs (scale bar = 20 nm) and histograms of metal particle size distribution for (a) Ir-ReO<sub>x</sub>/SiO<sub>2</sub> (2 wt% Ir, 2.2 wt% Re), (b) Pd-ReO<sub>x</sub>/SiO<sub>2</sub> (2 wt% Pd, 2.2 wt% Re) and (c) Pt-ReO<sub>x</sub>/SiO<sub>2</sub> (2 wt% Pt, 2.2 wt% Re).

**Fig. S6** FT-IR spectrum of pyridine adsorbed at 250 °C on Rh-ReO<sub>x</sub>/SiO<sub>2</sub> (2 wt% Rh, 2.2 wt% Re).

**Fig. S7** Conversion and selectivity in THFAM conversion to piperidine on Rh-ReO<sub>x</sub>/SiO<sub>2</sub> (2 wt% Rh, 1.4 wt% Re) for four reaction cycles. Reaction conditions: 1 mmol THFAM, 1 mmol HCl, 0.1 g catalyst, 10 mL H<sub>2</sub>O, 2.0 MPa H<sub>2</sub>, 200 °C, 3 h.

**Fig. S8** Transmission electron microscopy (TEM) micrographs (scale bar = 20 nm) and histograms of metal particle size distribution for the spent Rh-ReO<sub>x</sub>/SiO<sub>2</sub> (2 wt% Rh, 1.4 wt% Re) catalyst.

**Table S1** Turnover rate and selectivity in 5-amino-1-pentanol (APO) amination on various supported catalysts.

**General procedure for synthesis of N,N,N-trimethyl-1-(tetrahydrofuran-2-yl)methanaminium chloride.** N,N,N-Trimethyl-1-(tetrahydrofuran-2-yl)methanaminium chloride (TMTHFAM) was synthesized by treatment of THFAM with iodomethane in ethanol. Iodomethane ( $4.00 \times 10^{-2}$  mol) was added to an ethanol solution (20 mL) of THFAM ( $1.00 \times 10^{-2}$  mol) and sodium bicarbonate ( $3.00 \times 10^{-2}$  mol) with vigorous stirring at 25 °C. After reaction at 25 °C for 12 h, the resulting precipitate N,N,N-trimethyl-1-(tetrahydrofuran-2-yl)methanaminium iodide was collected by filtration, washing with diethyl ether and drying at 60 °C and ambient atmosphere. Afterward, N,N,N-trimethyl-1-(tetrahydrofuran-2-yl)methanaminium iodide was exchanged with 5.0 g Amberlite IRA402-Cl three times in water at 25 °C for 12 h. The reaction mixture was filtrated and the filtrate of TMTHFAM was evaporated to dryness at 65 °C under vacuum. The resulting powder TMTHFAM was dried in a vacuum at 60 °C.

$^1\text{H}$  and  $^{13}\text{C}$  NMR data for N,N,N-trimethyl-1-(tetrahydrofuran-2-yl)methanaminium chloride:  $^1\text{H}$  NMR (600 MHz, Deuterium Oxide)  $\delta$  4.48 (dt,  $J = 11.5, 5.7$  Hz, 1H), 3.93 – 3.80 (m, 2H), 3.50 – 3.42 (m, 2H), 3.18 (s, 9H), 2.23 – 2.13 (m, 1H), 1.99 – 1.83 (m, 2H), 1.60 (dq,  $J = 12.7, 8.0$  Hz, 1H);  $^{13}\text{C}$  NMR (151 MHz, Deuterium Oxide)  $\delta$  72.93, 69.38, 69.36, 69.34, 68.83, 54.11, 54.09, 54.06, 29.97, 24.49.

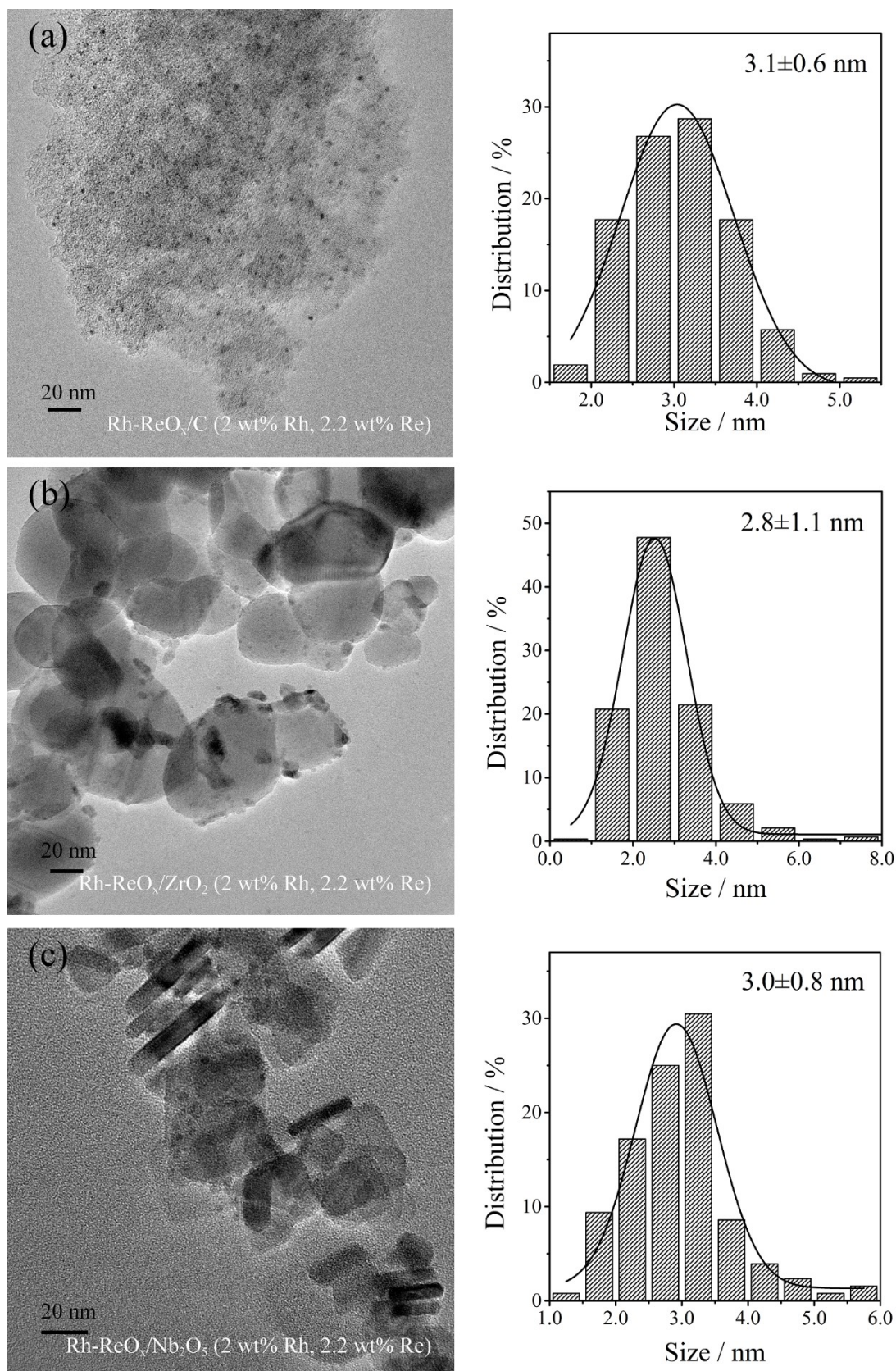


**Fig. S1** Transmission electron microscopy (TEM) micrographs (scale bar = 20 nm) and histograms of metal particle size distribution for (a) Rh-ReO<sub>x</sub>/C (2 wt% Rh, 2.2 wt% Re), (b) Rh-ReO<sub>x</sub>/ZrO<sub>2</sub> (2 wt% Rh, 2.2 wt% Re) and (c) Rh-ReO<sub>x</sub>/Nb<sub>2</sub>O<sub>5</sub> (2 wt% Rh, 2.2 wt% Re).

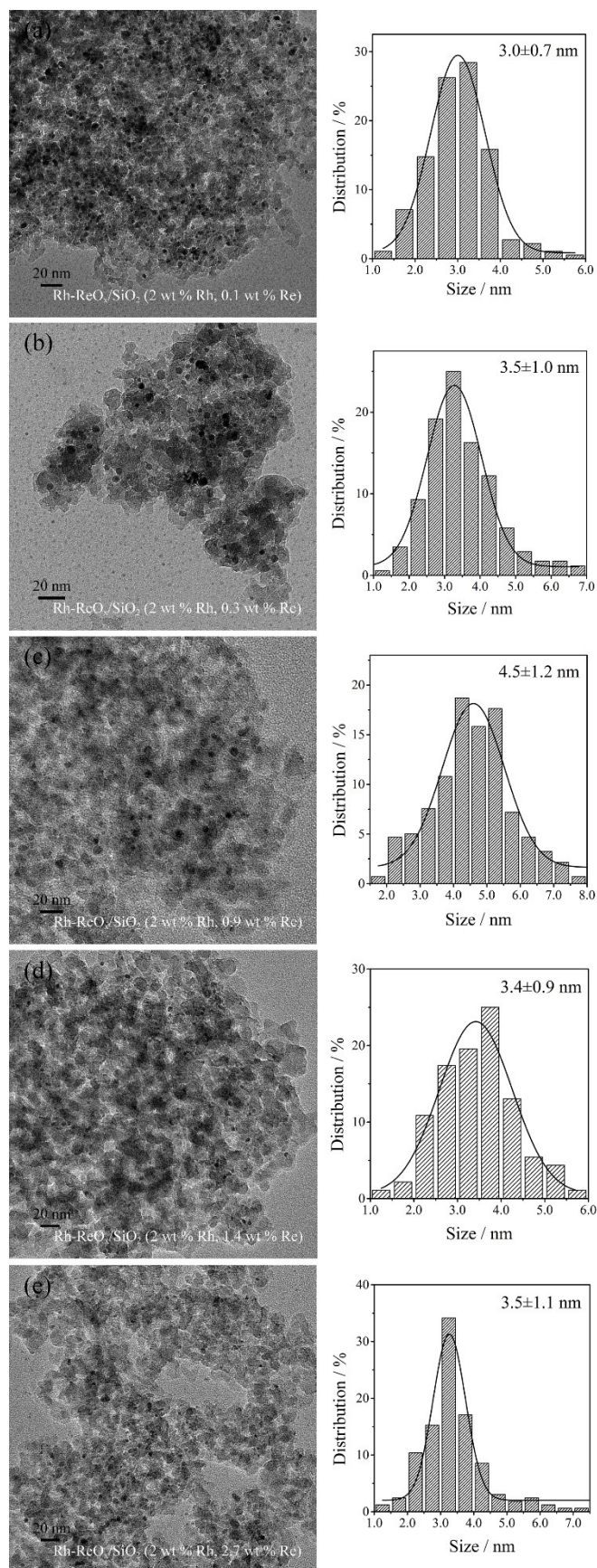


**Fig. S2** Transmission electron microscopy (TEM) micrographs (scale bar = 20 nm) and histograms of metal particle size distribution for Rh-ReO<sub>x</sub>/SiO<sub>2</sub> (2 wt% Rh, (a) 0.1 wt% Re, (b) 0.3 wt% Re, (c) 0.9 wt% Re, (d) 1.4 wt% Re and (e) 2.7 wt% Re).

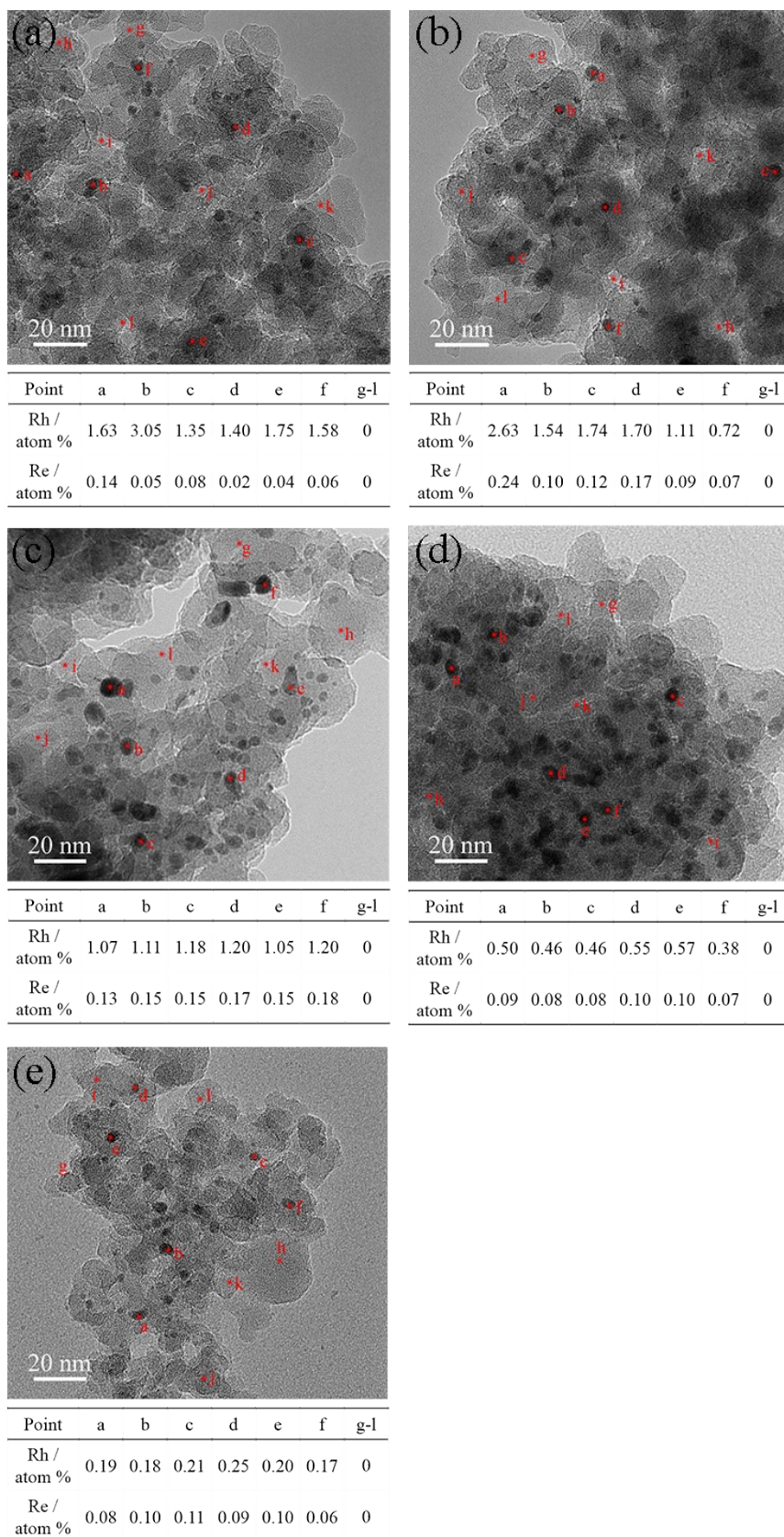


**Fig. S3** High angle annular dark field scanning transmission electron microscopy (HAADF-STEM) micrographs (scale bar = 20 nm) and electron dispersive X-ray (EDX) microanalyses of Rh-ReO<sub>x</sub>/SiO<sub>2</sub> (2 wt% Rh, (a) 0.1 wt% Re, (b) 0.3 wt% Re, (c) 0.9 wt% Re, (d) 1.4 wt% Re and (e) 2.7 wt% Re).

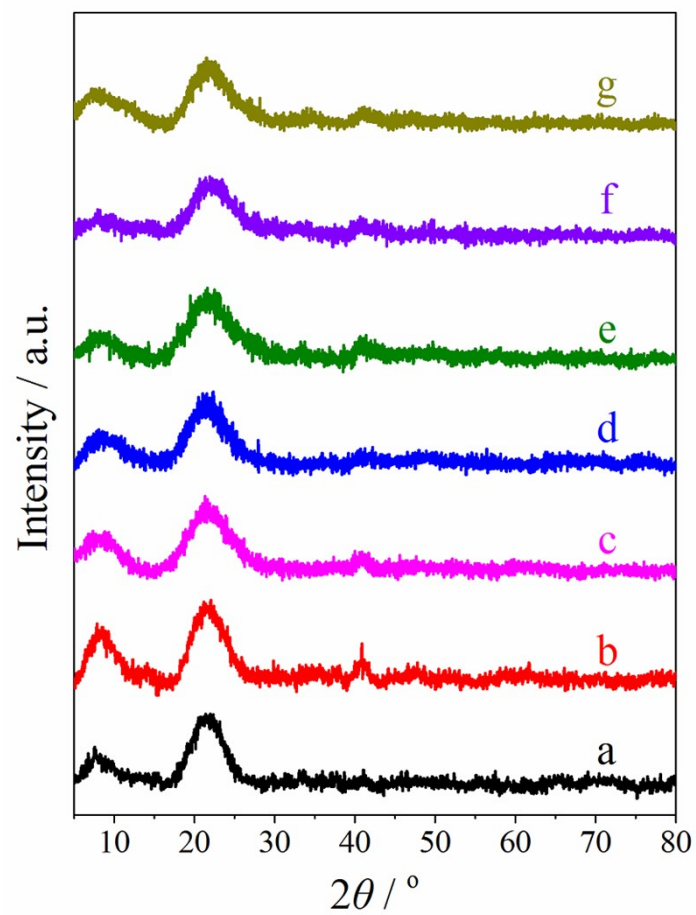


**Fig. S4** XRD patterns of Rh-ReO<sub>x</sub>/SiO<sub>2</sub> (2 wt% Rh, (a) 0.1 wt% Re, (b) 0.3 wt% Re, (c) 0.9 wt% Re, (d) 1.4 wt% Re, (e) 2.2 wt% Re, (f) 2.7 wt% Re) and (g) the spent Rh-ReO<sub>x</sub>/SiO<sub>2</sub> (2 wt% Rh, 1.4 wt% Re).

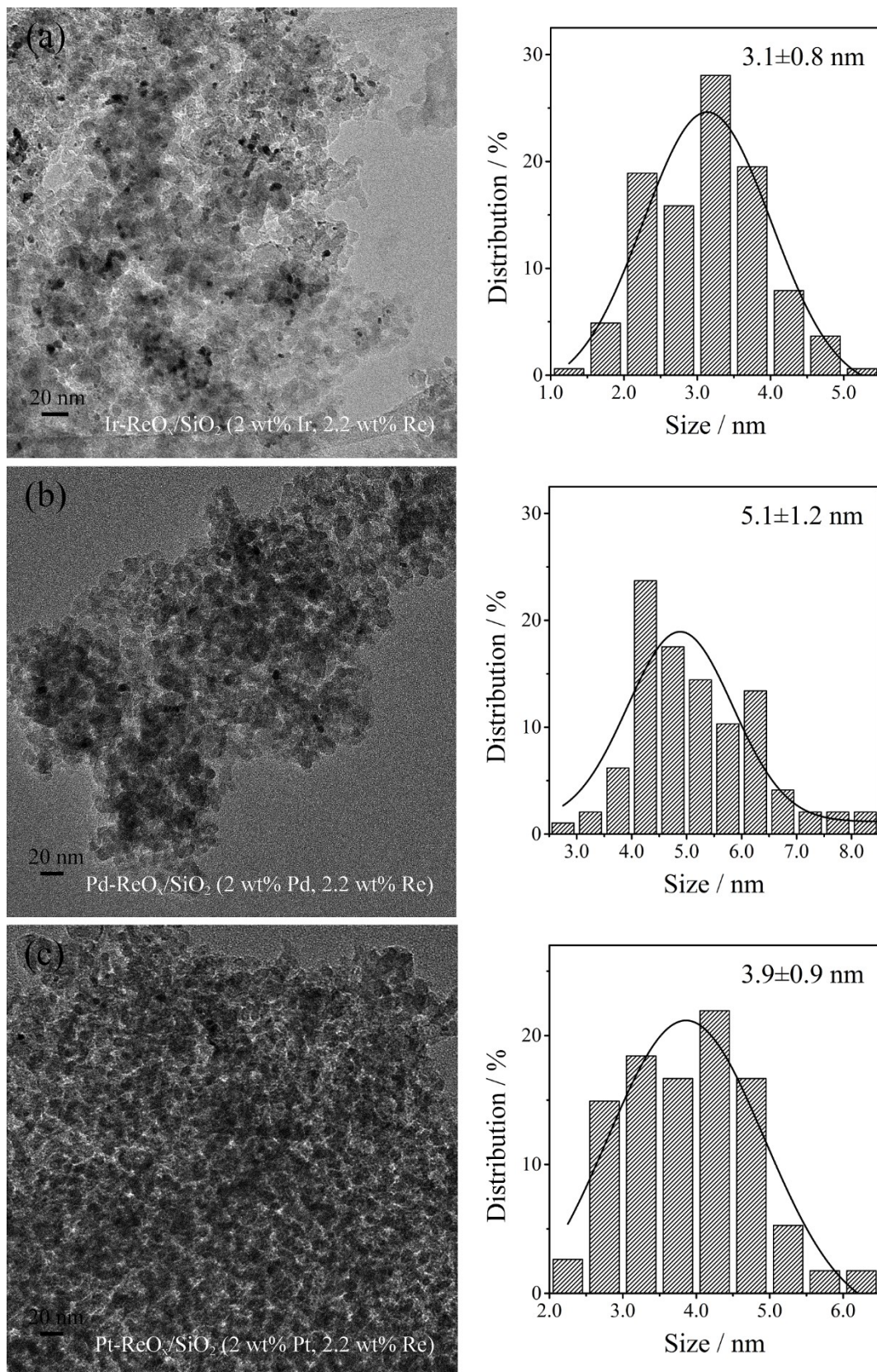


**Fig. S5** Transmission electron microscopy (TEM) micrographs (scale bar = 20 nm) and histograms of metal particle size distribution for (a) Ir-ReO<sub>x</sub>/SiO<sub>2</sub> (2 wt% Ir, 2.2 wt% Re), (b) Pd-ReO<sub>x</sub>/SiO<sub>2</sub> (2 wt% Pd, 2.2 wt% Re) and (c) Pt-ReO<sub>x</sub>/SiO<sub>2</sub> (2 wt% Pt, 2.2 wt% Re).

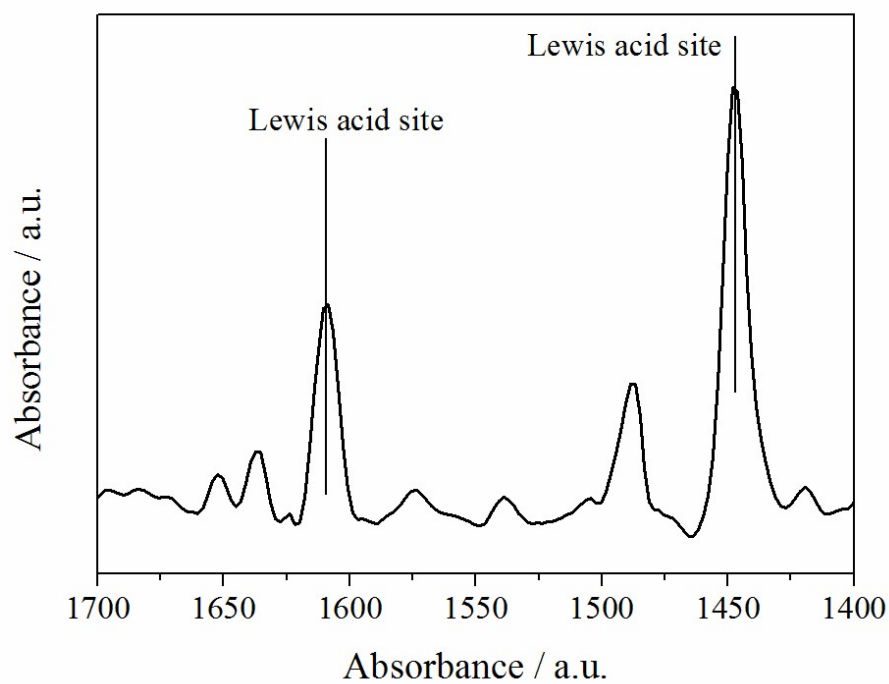


**Fig. S6** FT-IR spectrum of pyridine adsorbed at 250 °C on Rh-ReO<sub>x</sub>/SiO<sub>2</sub> (2 wt% Rh, 2.2 wt% Re).

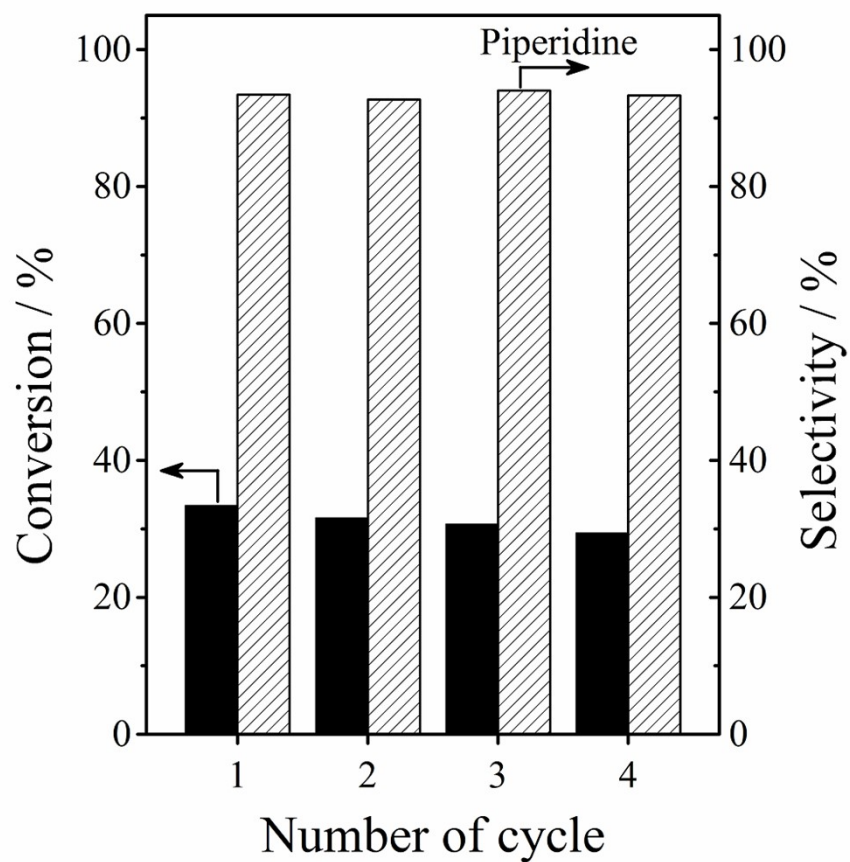


**Fig. S7** Conversion and selectivity in THFAM conversion to piperidine on Rh-ReO<sub>x</sub>/SiO<sub>2</sub> (2 wt% Rh, 1.4 wt% Re) for four reaction cycles. Reaction conditions: 1 mmol THFAM, 1 mmol HCl, 0.1 g catalyst, 10 mL H<sub>2</sub>O, 2.0 MPa H<sub>2</sub>, 200 °C, 3 h.

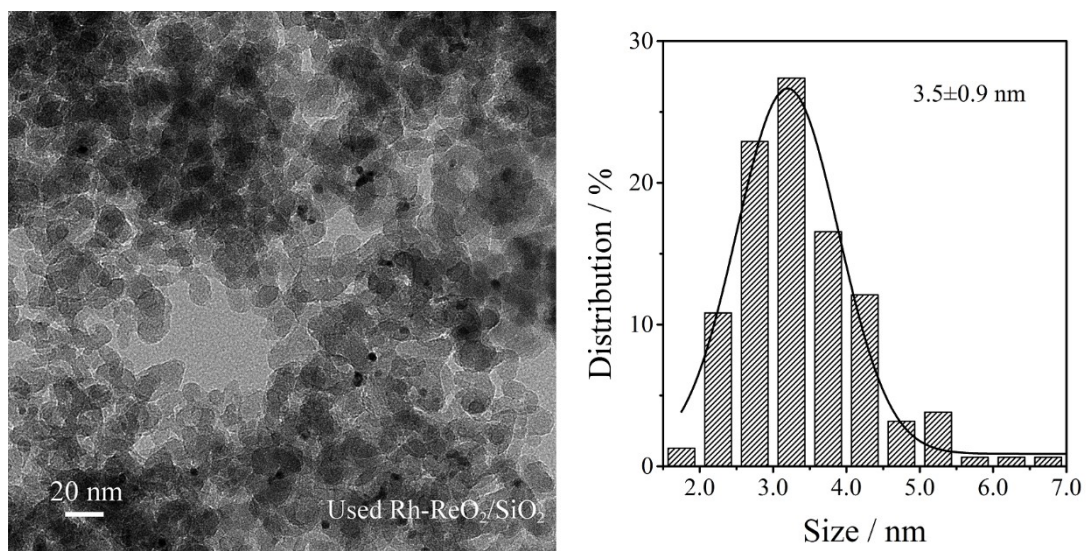


**Fig. S8** Transmission electron microscopy (TEM) micrographs (scale bar = 20 nm) and histograms of metal particle size distribution for the spent Rh-ReO<sub>x</sub>/SiO<sub>2</sub> (2 wt% Rh, 1.4 wt% Re) catalyst.

**Table S1** Turnover rate and selectivity in 5-amino-1-pentanol (APO) amination on various supported catalysts <sup>a</sup>

Entry	Catalyst	Turnover rate ( $\text{mol}_{\text{piperidine}} \text{mol}_{\text{surface-Rh}}^{-1} \text{h}^{-1}$ )	Molar selectivity (%)	
			Piperidine	Pentylamine
1	ReO <sub>x</sub> /SiO <sub>2</sub> (5 wt% Re)	0 <sup>b</sup>	-	-
2	Rh/SiO <sub>2</sub> (2 wt% Rh)	79.6	94.1	1.5
3	Rh-ReO <sub>x</sub> /SiO <sub>2</sub> (2 wt% Rh, 2.2 wt% Re)	152.5	97.4	0.7
4	Ir-ReO <sub>x</sub> /SiO <sub>2</sub> (2 wt% Ir, 2.2 wt% Re)	92.5	75.6	20.5

<sup>a</sup>Reaction conditions: 1 mmol APO, 1 mmol HCl, 0.05 g catalysts, 10 mL H<sub>2</sub>O, 2 MPa H<sub>2</sub>, 200 °C. 20-30% APO conversions obtained by varying reaction time. <sup>b</sup>No products were detected at 200 °C for 10 h.